Clim Dyn (2015) 44:3481–3491
DOI 10.1007/s00382-015-2485-5

Characterization of climatic zones, variability and trend in northern Africa

Zéphirin Yepdo Djomou · David Monkam · Roméo Chamani

Received: 22 February 2014 / Accepted: 14 January 2015 / Published online: 11 March 2015
© Springer-Verlag Berlin Heidelberg 2015

Abstract Using precipitation data from the Climatic Research Unit and the cluster analysis method, the northern Africa (0–30°N; 20°W–40°E) was sub-divided into four homogenous climatic zones for the base period (P0) 1901–1940. The four climatic zones were distributed into Saharan, Sahelian, wet tropical and equatorial climate types. The application of a segment of 15 years with overlap going from 1901–1940 (P0) and 1961 to 2000 (P4) throughout the periods 1916–1955 (P1), 1931–1970 (P2) and 1946–1985 (P3), shows important spatio-temporal modifications of rainfall zones south of 15°N. The semi-arid lands (Sahelian) which govern the dynamics of this zone doubled at the end of the twentieth century, while the wet tropical and equatorial zones decreased at the half. Temperature trends have a magnitude of up to 1.5 K per century in all the four climatic zones. This warming was mainly observed during the last three decades. During these same three decades, regional precipitation trends were less significant. The extreme conditions in temperature and the precipitation were analysed in terms of their persistence. The sporadic long-lasting extreme conditions appear for several years to over 10 years during the last century.

1 Introduction

Rainfall and temperature are frequently used to study climatic variability and change at local, regional and global scales. There have been many attempts to classify the spatiotemporal variability of North African rainfall. The number of regions and their locations significantly vary according to retained criteria and methodological approaches (Giorgi and Francisco 2000; Ward et al. 1999; Nicholson et al. 2000).

Hence, as in the past studies mentioned above, there are many criteria of the classification. This proves the complexity of climatic zonation and the difficulty to standardize regionalization criteria. African rainfall patterns have been analyzed in terms of either time or spatial zones since the early 1990s (New et al. 1999; Nicholson et al. 2008). These studies did not show the spatiotemporal variation of the climatic zones, otherwise there is no clear consensus for rainfall evolution at least over northern Africa. Furthermore, the trends of precipitation and temperature, is one of the most important and uncertain issues within the climate change research (New et al. 1999; Bell and Lamb 2006; Druyan 2010; Sarr 2012; Wang and Alo 2012). Therefore, we propose to revisit climatic zonation in northern Africa and try to bring out our contribution on how the spatio-temporal variation of the climatic zones could contribute to a better illustration and understanding of climatic changes in this part of the African continent. The main objective of the current work is to detect climatic zones and to study their spatial variability during the last century. In the next section, we describe the data and the methods used. In the third section, we present the results and conclusions are provided in Sect. 4.

2 Data and methods

The observation dataset was produced by the Climatic Research Unit (CRU) of the University of East Anglia, and it is described by New et al. (1999, 2000). For this study we

Z. Y. Djomou (✉) · D. Monkam · R. Chamani
Laboratory for Environmental Modeling and Atmospheric Physics, Department of Physics, Faculty of Science, University of Yaounde 1, P.O. Box 157, DRG Yaoundé, Cameroon
e-mail: ydjomou@yahoo.fr

use monthly surface air temperature and precipitation gridded on a regular latitude-longitude 0.5° global grid for the period of 1901–2000 (100 years). From the monthly surface air temperature and precipitation, annual and seasonal values are calculated and averaged in each climatic zone from January 1901 to December 2000. Only land areas are included in the dataset. New et al. (1999) provided estimates of the uncertainty associated with this climatology using both an internal cross-validation procedure and a comparison with other available observed climatologies. They concluded that uncertainties in observed climatic averages for multi-decadal periods are of the order of 0.5–1.3 K for temperature and up to 10–25 % for precipitation, and are largest over regions characterized by poor station coverage and high spatial variability, such as the African continent. Moreover the uncertainty and variability for earlier periods of the century may be amplified by even lower number of available stations. However, broad regional averaging tends to generally reduce the uncertainties associated with individual stations or periods. The analysis focuses on the December–January–Febuary (DJF), March–April–May (MAM), July–August–September (JAS) and yearly averaged (YAV) time series.

In this paper, cluster analysis (CA) (Wards method, squared Euclidean distance) is used to divide the northern Africa area (0–30°N; 20°W–40°E) in a number of climatically homogeneous zones based on the seasonal rainfall data for 267 grid points. CA has been applied to geophysical research during these two last decades (Gong and Richman 1995). It is among the most frequent methods used for statistical regionalization of geophysical fields such as rainfall (Champeaux and Tamburini 1994; Muñoz-Diaz and Rodrigo 2004, 2006; Crétat et al. 2012). CA generate a hierarchy of partitions of the data by successively merging (agglomerative) or splitting (divisive) of individual groups. Agglomerative methods consider all characteristics of the entity simultaneously, whereas divisive methods split them into subgroup at different stages of the procedure, a different criterion being used each stage (Gong and Richman 1995). This makes the computation speed of divisive methods show in particular when the number of entities to cluster is greater than about 100 (Mather 1976). All hierarchical methods perform the classification in five basic steps: (1) the chosen distance measured between entities is calculated; (2) the two closest entities are merged or split to form new clusters based on a defined criterion; (3) the distance between all entities is recalculated; (4) steps 2 and 3 are repeated until all entities are merged into one cluster (agglomerative) or all entities are split to form a cluster of its own (divisive). This gives a partition table of the classification called dendrogram; (5) a threshold is then applied to the dendrogram, the deduce the different clusters. Wards method is one of the most used clustering methodologies. In the present work, the CA is used to determine climatic zones on the base period 1901–1940 (P0).

To observe the spatio-temporal variations of the climatic zones, 15 years is added to the interval [1901–1940] boundaries of the base period P0 to obtain P1 [1916–1955]. Then 15 years is also added to the interval boundaries of P1 to obtain P2 [1931–1970]. The procedure is repeated until the period P4 [1961–2000] is obtained. This methodology permits to continuously track all the climate perturbations that occurred in the study area during the last century.

It is useful to briefly define some of the analysis measures used in this paper. The variability analysis is carried out on the monthly temperature and precipitation time series anomalies. Anomalies (*Ano*) are defined as the difference between the value (x) for a given year and the temporal mean ($\bar{x}$) of the field over the period of consideration. It is calculated by:

$$Ano = \frac{x - \bar{x}}{SD} \tag{1}$$

where SD explain the standard deviations.

One other measure that is used in the variability analysis is the persistence. To evaluate the persistence, the annual average of monthly anomalies must be computed. Then, the persistence is defined as the number of years experiencing similar sign of anomalies, i.e. if the anomaly changes sign from one year to the next the persistence is 1, if the sign change occurs after two years, it is equal to 2, etc. The persistence is thus a measure of how long anomaly regimes persist over the retained regions. Statistical significance throughout the paper is assessed using a t test at the 99 % confidence level.

Wavelet-based analyses involve the use of the continuous wavelet transform (CWT) (Kaiser 1994; Torrence and Compo 1998) of a time series function f(t). Since practically, the function f(t) consists of a discrete data set sampled at time steps δt, applying the convolution theorem the CWT can be interpreted as the inverse Fourier transform (FT) of the product of F(f(t)) and the FT of the scaled and translated basic function $F(\psi(s,\tau))$:

$$W_n(s) = \sum_{k=0}^{N-1} \hat{f}_k \bar{\hat{\psi}}_s(sw_k) e^{iw_k n\delta t} \tag{2}$$

where $\hat{}$ indicates the Fourier transform, n the localized translated time, k the frequency index and $w_k = \pm\frac{2\pi k}{N\delta t}$ the angular frequency.

In this study Morlet wavelet is used, which is a complex wave attenuated by a Gaussian (the non-dimensional frequency is set to $w_0 = 6$) and the dyadic set of scales $s_j = 2\delta_j 2^{j\delta_j}, j = 0, 1, \ldots, J$.

The scale averaged wavelet spectrum which describes the time series variance within a selected scale band is

obtained by averaging the local wavelet coefficients along the N-vertical cuts of the time axis:

$$\bar{W}_n^2 = \frac{\delta j \delta t}{C_\delta} \sum_{j=j_1}^{j_2} \frac{|W_n(s_j)|^2}{s_j}, \qquad n = 1, \ldots, N \tag{3}$$

where C_δ is a scale independent characteristic of the basic function used (Torrence and Compo 1998).

The average of the wavelet power over all local wavelet spectra along the time axis is called the global wavelet spectrum (GWS) (Torrence and Compo 1998):

$$\bar{W}^2(s) = \frac{1}{N} \sum_{n=0}^{N-1} |W_n(s)|^2 \tag{4}$$

Significance of the periods observed by the GWS is tested by the χ^2 test (Torrence and Compo 1998) and the random permutation shuffling procedure.

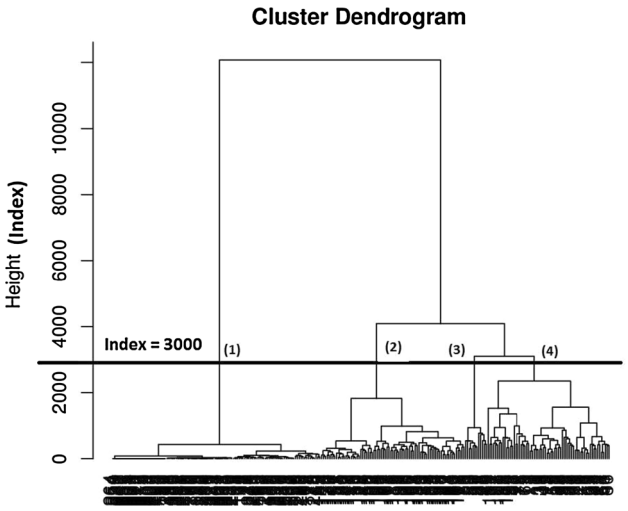

Fig. 1 Dendrogram obtained from the CA method applied on July to September (JAS) rainfall data in northern Africa

3 Results

3.1 Climatic zones

Figure 1 illustrates the dendrogram obtained from the CA method applied on July to September (JAS) rainfall monthly anomalies of the base period. This dendrogram shows different groupings of n observations at each of the $n - 1$ steps. At the first step, each observation is in a separate group and after the last step all the observations are in a single group. An important practical problem in CA is the choice of which intermediate stage will be chosen as the final solution. One approach to the problem of choosing the best number of clusters is through the level of aggregation in the dendrogram to stop the merging of clusters (cutting index). The dendrogram indicates the order in which, successive aggregations were operated. It also indicates to us the value of the aggregation index at each aggregation level. In practice the cutting of the dendrogram is done after aggregations corresponding to relatively low values of the index and before aggregations corresponding to high values of the index. By cutting the dendrogram at the significant jump level of this index, we hope to obtain good quality partition because, aggregated clusters below the cutting are very closed, and those aggregated after the cutting are very distant.

In this case (Fig. 1), the minimum and the maximum indices are at 0 and 12,000, respectively. From an index greater than 4,000 the aggregated clusters are very distant while for an index below 2,000 the aggregated clusters are rather close. So, the best cutting index is between 2,000 and 4,000. The medium index value of this interval is at 3,000 and corresponds to the cutting index. The horizontal line at this index has four intersection points (1), (2), (3) and (4) with the dendrogram (Fig. 1). If the horizontal line is displaced between 2,000 and 2,500, there will be 5 intersection points, while between 1,800 and 2,000 the number of intersection points is 6. If the displacement of the horizontal line below the index 2,000 continues, the number of intersection points with the dendrogram will increase and consequently the number N of climatic zones: N = 5, 6, 7, 8, etc. Therefore, for this study, the number of clusters is 4 corresponding to the cutting index 3,000. To confirm the choice of N = 4, we proceeded to the zonation with N = 5, 6, 7 and 8 climatic zones (figure not shown). For the case of 5 climatic zones, we note that GI occupies two spaces; GIV occupies five spaces and GV two spaces. For the case of 6 climatic zones, we note that GI occupies two spaces, GII two spaces; GIV occupies two spaces, GV three spaces and GVI two spaces. Thus, as the number of climatic zones increases, the number of spaces occupied by these climatic zones increases or decreases. Finally for this study zone, the climatic zones are not homogenous with N greater than 4.

Thus Fig. 2 displays four zones on six areas for the base period (1901–1940). The first zone (GI) occupies 2 areas. It includes mainly the Sahara and a small area east of Lake Rudolph in Kenya. This small area has a strong spatial inhomogeneity resulting from the local topography and the land cover vegetation map in northern and southern Africa (Dreiser 1994; Nicholson 2000, 2001; Kaptué et al. 2010, 2011). Similar results, where the analysis put two areas in the same cluster, were also obtained by Penlap et al. (2004) when they analyzed possible changes in precipitation in Cameroon. The second zone (GII) is centered on the South of Chad, with almost regular extension to the west towards Mali, and to the east, including central and southwestern

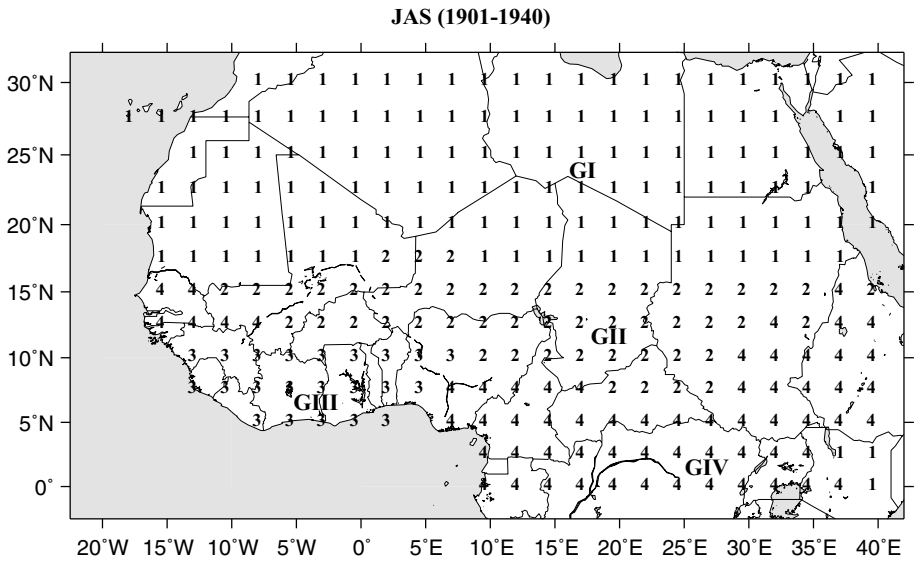

Fig. 2 Climatic zones of JAS season for the base period P0 (1901–1940)

Sudan. The third zone (GIII) is described the Guinean coast region. The fourth zone (GIV) contains two areas geographically different with one over Senegal while the other covers the south of Sudan and a part of Ethiopia and Uganda. This zone is widely extended and covers entirely the Central Africa.

The comparison of our results with the works of Janicot (1992) and Giorgi (2002) shows good similarities. Janicot (1992) considered the period 1948–1978 and also found four zones. Three of the four zones are very similar to GII, GIII and GIV described above (Fig. 2). Janicot (1992) did not extend his study area north of 20°N, over the Sahara corresponding to GI here. Giorgi (2002) also shows that northern Africa is divided into three climatic zones. These three climatic zones are very similar to GI, GII and GIII described above (Fig. 2). We also compare our results to the African Atlas (2000) zonation. In this atlas, the African continent is divided into 6 climate types distributed symmetrically around the equator as equatorial, humid tropical, dry tropical, Sahelian, desert and Mediterranean climate types. Except for the Mediterranean, our study area contains 5 of these 6 climate types. One of our zones contains the two tropical climate types. In both regionalizations, the zones have the same overall tendency, with zonally extended bands. We also, analyse the trend in all those four climatic zones. The trends of time series of temperature and precipitation anomalies are analyzed, over the four climatic zones during the last century (see Sect. 3.3). It is evident from both temperature and precipitation that trends are not the same in all the four climatic zones. For instance, the precipitation trend in the Sahara (GI) is linear (i.e. harmonic is observed with very weak amplitude) whereas in the other climatic zones, the harmonics are observed with very high amplitudes. Also, the harmonic amplitudes are not the same in the three other climatic zones. In GIII, we observed a substantial variability trend than in GII and GIV. The CA method as we used here contributes not only to identify the climatic zones, but also to detect the variability of those climatic zones through the area during a given period. The rainfall anomalies zonation and their temporal variability, contribute to illustrate climate variability. In the following sections, we analyse the trends in each climatic zone and we apply the CA method on the four periods PI, PII, PIII and PIV described in Sect. 2, to study the spatio-temporal variability of these climatic zones during the last century.

3.2 Spatio-temporal variability of climatic zones

The spatio-temporal evolution of the climatic zones is clearly visible on Fig. 3 presenting the zones for the periods PI, PII, PIII, PIV. By using the 15-year moving-period, the modifications of each cluster between each period are as follow:

From the base period (1901–1940) to the end of the century, GI and GII show an extension (PIII and PIV for GI: Fig. 3c, d; PI, PII and PIV for GII: Fig. 3a, b, d) through the intermediate period of shrinking (PI and PII for GI: Fig. 3a, b; PIII for GII: Fig. 3c). This extension of GI and GII is done at the detriment of GIII and GIV which are respectively shrunk and confined on the south-east of Liberia and the Gulf of Guinea at the end of twentieth century. The spatio-temporal evolution of the climatic zones is observed by a shrinking for some and an extension for others.

There is an expansion of climatic zones GI and GII during the last 40 years of the twentieth century. This result of the evolution of climatic zones is confirmed by the surface computations shown in Table 1. In Table 1, there appears

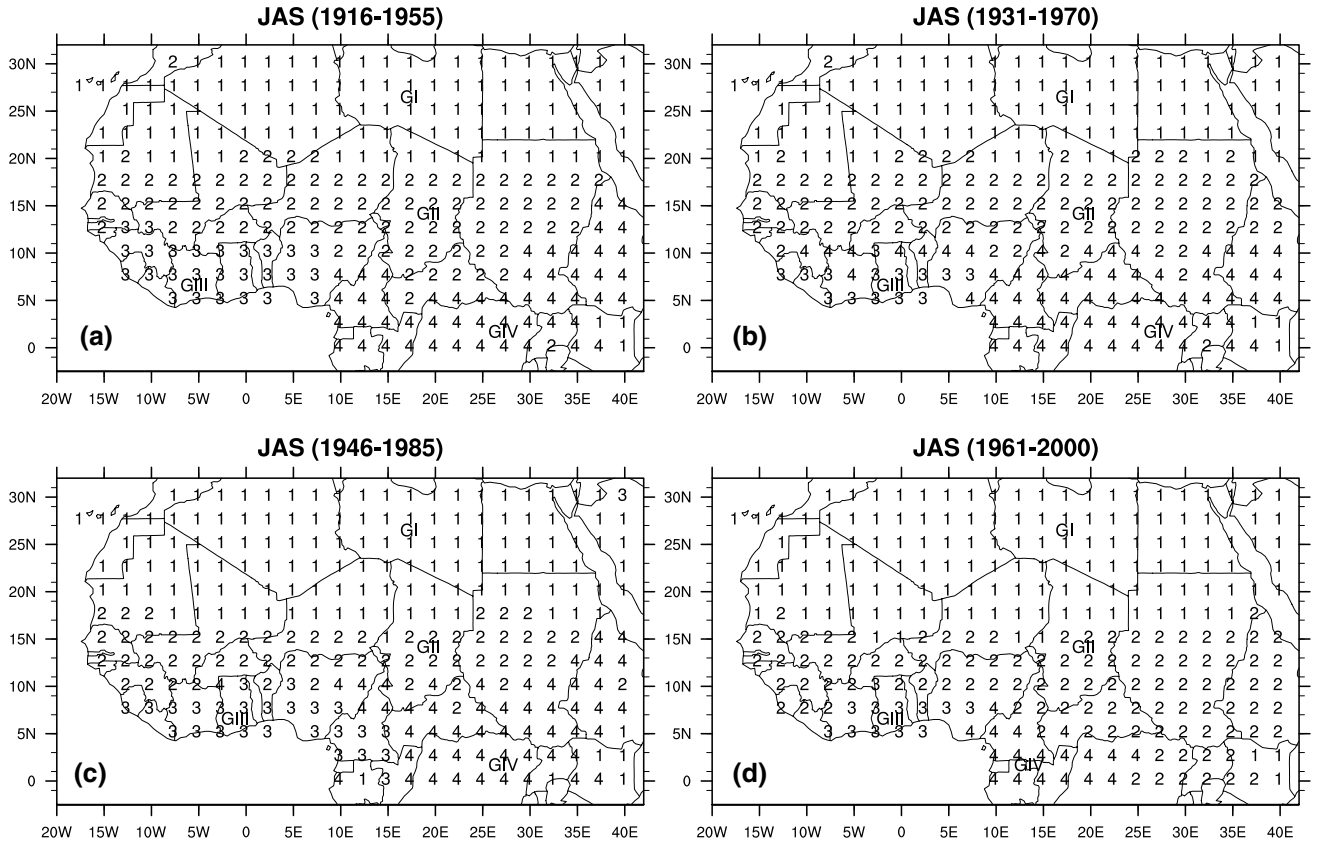

Fig. 3 Climatic zones evolution of JAS season during 1901–2000. The basic state is identical as the Fig. 2 and one can note the extension of GII during the last century

for each climatic zone and period the surface and the mean rainfall per unit area (MRUA). To obtain the MRUA in a climatic zone, the mean rainfall is computed at each grid point for a given period. Then the sum is computed for all the grid points of the climatic zone and the result is then divided by the surface of the climatic zone. The time variation of MRUA is very weak in GI and its fluctuations are also weak during the century. This quantity slightly increases in GII and decreases in GIII and GIV during the century.

In general, the surfaces of GIII and GIV decrease during the century. On the contrary, the surfaces of GI and GII increase. In the base period, GI and GII occupy about 68.56 % of the total study area, GIII and GIV cover only 31.44 %. At the end of the century, the area percentage of GI and GII is 88.76 % whereas that of GIII and GIV is 11.24 %.

The changes observed in northern Africa could be related to large-scale atmospheric changes as well (not studied here). Halpert and Ropelewski (1992), Ropelewski and Halpert (1996) and Hurrell (1995) showed that over northern Africa, the ENSO and NAO likely influence the interregional temperature and precipitation. We can also mention that the regional temperature and precipitation anomalies from CRU data as well as the SOI and NAOI have non-stationary character (Giorgi 2002). This could influence the stability in time of the relationship between ENSO and NAO. There is also one of the most important spatial pattern forcings of African

Table 1 Evolution for climatic zones surface (surf) in 10^6 km^2 and the mean rainfall per unit area (MRUA) in mm/km^2 over northern Africa during the twentieth century

Region	1901–1940		1916–1955		1931–1970		1946–1985		1961–2000	
	Surf	MRUA	Surf	MRUA	Surf	MRUA	Surf	MRUA	Surf	MRUA
GI	10.16	0.85	8.32	0.30	7.93	0.28	10.09	0.90	10.55	1.05
GII	3.93	16.93	6.24	14.72	6.55	13.90	4.39	18.90	7.70	21.24
GIII	1.69	30.10	2.00	31.05	1.08	27.43	1.93	27.48	0.92	20.00
GIV	4.78	22.83	4.00	21.20	5.01	24.30	4.16	22.00	1.39	24.18

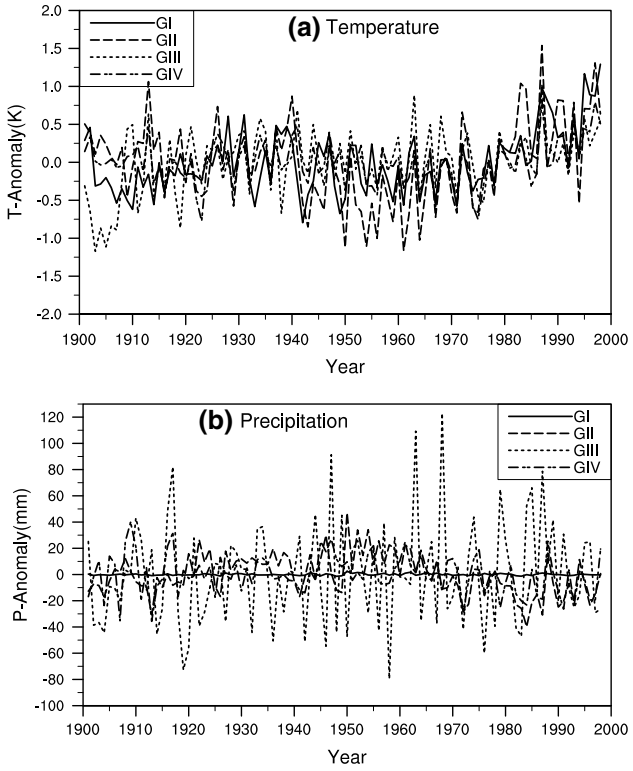

Fig. 4 Time series of seasonal (JAS) average temperature (T) and precipitation (P) anomalies for the twentieth century over the four climatic zones. Units are K for temperature and in mm for precipitation. The anomaly is calculated with respect to the 100-year average

tropical rainfall regime called "dipole" (not studied here). Thus, the strong pressure anomalies in the tropical North Atlantic and the South Atlantic in the wet and dry composites suggest links to more global phenomena. The former sector is involved in the NAO (Czaja et al. 2002). However, the NAO is linked to the tropical Atlantic mainly during the boreal winter, and in fact it may be forced by the tropical Atlantic (Robertson et al. 2003). Nevertheless, the strength of the anomalies suggests that possible relationships with the NAO should be further investigated. Also, the South Atlantic has been identified as a possible source of remote forcing for tropical Atlantic variability (Rajagopalan et al. 1998; Venegas et al. 1997; Tourre et al. 1999; Mo 2000; Mo and Hakkinen 2001; Hickey and Weaver 2004) and African rainfall variability (Camberlin et al. 2001). It appears prominently in the reconstruction of links to the Pacific ENSO (Nicholson 1997; Nicholson and Kim 1997) and in the contrast between wet and dry years in western central Africa (Balas et al. 2007) and southern Africa (Nicholson 1989).

3.3 Regional trend analysis

Figure 4 presents the time series of temperature and rainfall anomalies, over the four climatic zones during the last century. Anomalies are calculated with all the 100-years rather than the trend line in order to show trends throughout the century. It is evident from Fig. 4 that both temperature and precipitation are characterized by substantial variability at time scales from several years to multi-decadal.

For the temperature, we find periods of warming in the first 3–4 decades and the last 2–3 decades, separated by cooling in the intermediate decades in all the four climatic zones. Most climatic zones show a general trend of increasing temperature throughout the century, consistent with the observed warming trend found at the global scale (Jones et al. 1999; Giorgi 2002). The results exhibit warming trends in the range of 0.5–1.5 K per century.

Seasonal precipitation anomalies slightly vary over the Sahara desert (GI), whereas the other climatic zones, and particularly zone GIII present fluctuations during the last century where the precipitation decrease and the temperature increase since 1970s. GI and GIV show the negative anomalies since the 1970s. Seasonal precipitation trends can be associated with shifts in general circulation features such as African monsoon circulation or with changes in the thermodynamic structure of the atmosphere. The African monsoon system is one of the main factors which determine the state of the weather in northern Africa. Thus, precipitations variability is subject to the African monsoon movement in northern Africa during the year (Sultan and Janicot 2003; Mounier et al. 2008). Also, the large scale-effect such as sea surface temperature (SST) determines the state of weather in northern Africa. The 1950–1999 time period of northern Africa rainfall during their respective wet seasons are well described by linear downward trends (Hoerling et al. 2006). A correlation of each time series with SSTs suggest that drying over this region has similar oceanic ties. A striking common feature is the warm SSTs throughout the Tropics associated with drying during both seasons, a pattern resembling the 1950–1999 SST trend pattern itself (Giannini et al. 2008; Hoerling et al. 2006; Biasutti et al. 2008).

By observing this correlation between rainfall and SST, one can explore the nature and causes of the regional downward trajectories of African rainfall. One question is that: are these drying trends consistent with natural variability alone, in particular the intrinsic variations of the coupled oceanatmosphere system? Unfortunately, this aspect was not approached within the framework of this study. But, Hoerling et al. (2006) in their study concluded from climate model experiments that the late twentieth century drying trend over the Sahel was likely due to natural causes and has not been a harbinger for human induced climate change of oceanic origins. Also, Giannini et al. (2008) concludes that the atmospheric models driven by the observed long-term history of global sea surface temperature (SST) reproduced the timing and decadal time scale of change in Sahel

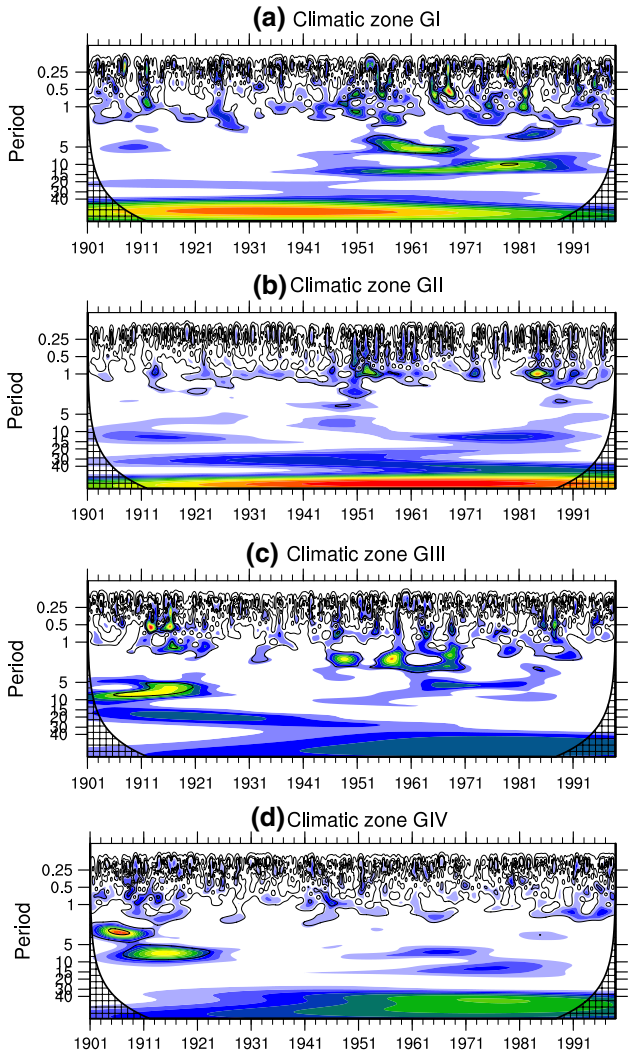

Fig. 5 Wavelet power spectra using Morlet wavelet for the time series of yearly average precipitation anomalies for the twentieth century over the four climatic zones (Fig. 2) in northern Africa. The *solid line* drawn through the wavelet spectra delineates the cone of influence

rainfall, the shift from anomalously wet to persistently dry that occurred at the end of the 1960s, as well as its spatial extent from the Atlantic coast (Giannini et al. 2008).

Figure 5 shows the power spectra of the transformed wavelet for the time series of yearly average precipitation anomalies in the northern African region (Fig. 2), which is a record of 100 years. Wavelet analysis is a common tool widely used for analyzing, localized variations of power within a time series. By decomposing a time series into timefrequency space, one is able to determine both the dominant modes of variability and how those modes vary in time. As stated before, the transformed wavelet gives information on the relative power at a certain scale and a certain time over all the four climatic zones in northern Africa. Figure 5 shows the actual oscillations of the individual wavelets, rather than just their magnitude. The solid line drawn through the wavelet spectra delineates the cone of influence. For the four climatic zones, the wavelet power spectrum shows the timescale of variability which is governed by 3 main periodicity bands: <5 years, from 5 to 30 years and above 30 years.

Observing Fig. 5a (climatic zone GI), the wavelet power spectrum illustrates clearly the significant peaks whose periods are concentrated between the 0.25–15 yearly band. The significant energy below 1 year is observed at the beginning, the medium and the end of the twentieth century. The presence of significant peaks around 3 years is observed between 1978 and 1987. After the 1955, the significant wavelet power spectra is observed around 5 years and around 10 years which reflects the substantial variability at time scale from several years to multi-decadal shown in Fig. 4b. This is also performed to document the analysis of the persistence of the extreme conditions of precipitation (see Sect. 3.4).

For the climatic zone (GII) (Fig. 5b), precipitation signal exhibits variability mainly in the periodicity bands of <5 years. The strongest significant signal can be found around 1 year periodicity in 1914, 1946, 1973, 1991 and the interval [1949–1959], [1983–1987], some low but significant peaks also appear around periods of 2 years ([1949–1952], [1985–1996]), 3 years ([1919–1924], [1947–1954]) and 4 years ([1945–1952], [1987–1991]). As in zone GI, GIII shows the significant energy below 1 year at the beginning, the medium and the end for the entire record (Fig. 5c). Significant signals are also observed in the band 1–5 years ([1914–1919], [1946–1971]) and band 5–10 years ([1903–1921]). The significant signal from 1 to 10 years also shows the substantial variability at time scale from several years to multi-decadal as illustrated in Fig. 4b. As stated before, the band 1–10 years reflected the persistence of the extreme condition of precipitation analysed in Sect. 3.4. As for the previous three regions, the timescales of GIV (Fig. 5d) under 1 year are significant for the entire record. The strongest power is located in the band 3–5 years (1901–1911) and in the band 5–10 years (1907–1921).

Finally, the significant signal from 1 to 10 years which reflects the substantial variability at time scale from several years to multi-decadal, documents the analysis of the persistence of the extreme condition of the precipitation described in Sect. 3.4.

GIV (Fig. 5d): for this climatic zone, as for the climatic zones GI and GIII, the significant precipitation variability timescales are located in the band of periodicity of < 10 years. As for the previous three regions, the timescales under 1 year are significant for the entire record. The strongest power are located around 4 years (from 1901 to 1912) and in the band 5–10 years (from 1907 to 1923). As

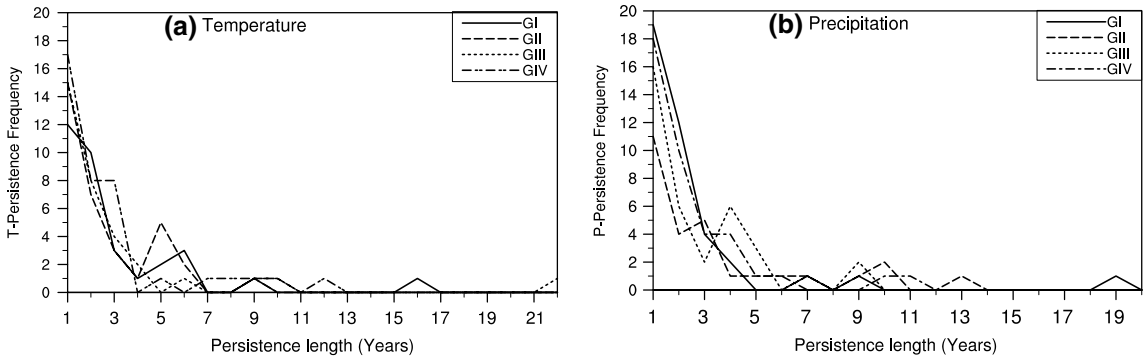

Fig. 6 Persistence frequency as a function of length (years) for temperature (T) and precipitation (P) YAV anomalies over northern Africa

Table 2 Number of persistence length >3 years for regional temperature (T) and precipitation (P) during the period 1901–2000 in the observed record

Region	T				P			
	DJF	MAM	JAS	YAV	DJF	MAM	JAS	YAV
GI	1 (9)	1 (16)	1 (16)	1 (16)	1 (12)	1 (12)	1 (6)	1 (19)
GII	1 (8)	2 (11)	1 (11)	1 (10)	2 (6)	1 (9)	1 (13)	1 (13)
GIII	1 (16)	1 (10)	2 (6)	1 (22)	1 (9)	2 (5)	2 (6)	2 (9)
GIV	1 (20)	1 (16)	1 (8)	1 (12)	1 (11)	1 (9)	1 (6)	1 (10)

Length in years of the longest persistence shown in parentheses

we observed above, the 2–10 years band documents the analysis of the persistence of the extreme condition of the precipitation described in Sect. 3.4. In this climatic zone, the strong oscillation is observed only during the two first decades (1901–1921).

3.4 Regional persistence analysis

An analysis of the persistence and frequency of the temperature and precipitation anomalies (see Sect. 2) is performed to demonstrate not only the statistical distribution of the anomalies, but also the occurrence of extreme conditions and long-lived regimes.

Example of persistence distribution of yearly average (YAV) temperature and precipitation de-trended anomalies as a function of time length is shown in Fig. 6. In general, the persistence rapidly decreases with length. For most climatic zones, the sign of the anomaly changes from one year to the next about 11–17 times for temperature (Fig. 6a) and 10–19 times for precipitation (Fig. 6b) throughout the century. Anomaly persistence of two years is found 6–10 times for temperature and 4–13 times for precipitation, while anomaly persistence of three years occurs 3–8 times for temperature and 3–5 times for precipitation, etc. Table 2 shows for each zone, the occurrence of persistence greater than 3 years along with the longest persistence found in the time series. Long persistences for both temperature and precipitation occur from 1 time to 2 times during the century, and many cases of persistence exceeding 10 years can be observed. These are related to the establishment of multi-year regional anomaly regimes influencing given climatic zones whose effect is greater than the superposed year-to-year variability. For example, the longest persistence (22) is found over the Gulf of Guinea zone (GIII) for YAV temperature and corresponds to a multi-decadal period of relatively high temperature that occurred between the early 1940s and the end of the century (see also Fig. 4a).

Table 2 shows that, overall, temperature tends to exhibit longer persistence exceeding 10 years over all climatic zones, especially Gulf of Guinea (GIII) and Sahara (GI). We can also underline the 4 wet years (1958–1961) and 4 dry years (1982–1985, 1969–1972) (Nicholson and Grist 2001) which can influence the long persistence observed in northern Africa. The possible physical explanations of persistence would be the global or the local factors. Rowell et al. (1995) and Ward (1998) effectively demonstrated strong contrasts in spatial tele-connections and SST associations in high and low frequency variabilities. Nicholson and Grist (2001) model is compatible with this framework, but it focuses on the links between rainfall and local atmospheric processes over Africa, rather than the SST-rainfall associations and tropical tele-connections. It is also

compatible with the suggestion of Nicholson (1989) and Zeng et al. (1999), that dynamic factors trigger major shifts in the Sahel (GII) rainfall regime, while land atmosphere feedback (deforestation, drought, desertification) tends to promote the persistence of these regimes.

4 Discussion and conclusions

The main objective of the present work was to study the dynamic evolution of the climatic zones, the variability and the trend in northern Africa. We produced the climatic zones and studied their spatio-temporal variability during the last century, thereafter, we analysed the trend and the persistence of temperature and precipitation in northern Africa.

The main results of this analysis can be summarized as follows:

Significant century-scale warming trends of magnitude up to 1.5 K per century are observed over the majority of climatic zones, although the structure of the temporal series varies considerably across zones. The largest trends are found over wet land region (GIV), likely as result of the deforestation albedo feedback mechanism (Giorgi 2002). Only GII and GIV zones show significant century-scale trends in precipitation, mostly negative sign at the end of the twentieth century.

The spatio-temporal evolution of all the four climatic zones has been shown through the extension of dry climate zone (Sahara and Sahel) and the reduction of wet climate zone (Equator). The precipitation decrease was associated with the temperature increase mainly after the 1970s. Particularly, the zone GI which corresponds to the desert climate with weak precipitation has been subject to a slight extension toward the south. This situation contributes to desert extension. For zone GII which corresponds to the Sahelian climate which is less warm than the desert, its extension was more marked during the last century. GII is impacted by the monsoon during boreal summer. GII is also, the main area of squall line occurence during northern summer and it is located slightly north of 10°N (Nicholson et al. 2000; Janicot 1992; Yepdo et al. 2009). The zone GIII is located between 10°N and the Guinea coast. It is the region of monsoon rainfall during northern summer. This latitude of 10°N boundary between zones GII and GIII was also noted by Nicholson et al. (2000) and Janicot (1992). The last author analysed the Sahelian rainfall for the period 1948–1978. He found that the intertropical convergence zone (ITCZ) mean position was southern (10°N) than the normal in summer. The interannual variability of the divergent meridional circulation (Hadley cells) is responsible of the West Africa rainfall variability, and was examined by Fontaine and Janicot (1992). The progression of the zone GII during the period, P4, can be explained by the southern position of the ITCZ that could be linked to a less vertical continuity of Hadley and Walker cells over Sahel during the dry period 1968–1975 as was mentioned by Janicot (1992). Between the beginning (1901–1940) and the end (1961–2000) of the century, this progression of GII has substantially reduced zones GIII and GIV by about 50 %. Finally, the semiarid land has widely grown during the twentieth century.

The sign of the anomaly tends to change from one year to the next at a frequency similar to that of a random series. However, instances occur in which the same anomaly sign persists for several years to over 10 years. This suggests a picture of a chaotic-type behaviour in which regional conditions oscillate around the mean trend and occasionally fall into relatively stable and long-lasting anomaly regimes (e.g., Corti et al. 1999).

These regimes can also be affected by internal oscillations of the climate system such as the El Niño Southern Oscillation (ENSO) and the North Atlantic Oscillation (NAO) (e.g. Hurrell 1995). Hoerling et al. (2006) in their study concluded starting from the climate model experiments that the late twentieth century drying trend over the Sahel was likely due to natural causes and has not been a harbinger for human induced climate change of oceanic origins. Also, Giannini et al. (2008) concludes that the atmospheric models driven by the observed long-term history of global sea surface temperature (SST) reproduced the timing and decadal time scale of change in Sahel rainfall, the shift from anomalously wet to persistently dry that occurred at the end of the 1960s, as well as its spatial extent from the Atlantic coast (Giannini et al. 2008). By observing all these research results, it is expected that further diagnosis of physical processes underlying the tele-connective response of African climate to SST forcing will be a challenge.

Other modeling studies have tackled the question of whether they should attribute the twentieth-century Sahel droughts to internal climate variability or to anthropogenic emissions of greenhouse gases and aerosols (Biasutti et al. 2008). Rotstayn and Lohmann (2002) and Hoerling et al. (2006), following Folland et al. (1986) and others, have both emphasized the role of the differential warming of the Northern and Southern Hemispheres in determining the meridional location of the Atlantic ITCZ and the extent of the West African monsoon. The former study, however, argued for the role of anthropogenic aerosol in forcing Sahel drought, and the latter argued for natural variability (Biasutti et al. 2008). Also, Biasutti and Giannini (2006) in their Coupled Model Intercomparison Project 3 looked at Sahel rainfall variations and they showed that at least 30 % of the observed negative rainfall trend over the 1930–2000 period was estimated to be externally and most likely anthropogenically forced. They

concluded that although the role of internal climate variability was predominant in forcing the sharp decline in Sahel rainfall in the 1960s and 1970s, anthropogenic influences have also been substantial, giving reasons to worry about the future. Also, today there is sufficient evidence of rising global temperatures due to increased emission of greenhouse gases (Carbon dioxide, Nitrous oxide, Methane and Chlorofluorocarbons) into the atmosphere. The increased global warming has the capacity to trigger large-scale climatic disturbances, which ultimately may have significant impact on the Sahel rainfall (Biasutti and Giannini 2006). In spite of this, no satisfactory explanation has yet been offered for the causes of the West African sahelian drought, although scientists agree that the causes are primarily related to large-scale patterns of atmospheric circulation.

The evolution of climatic zones by using zonation and projection data of twenty-first century could also be employed to monitor changes in future years (not studied here). May be, the extension of the semi-arid zone observed during the last century could continue into the 21st century. This could be used for instance, to make projections in order to facilitate forward planning policies related to agricultural land management and hence in arable land.

Acknowledgments We would like to acknowledge the constructive comments and suggestions of two anonymous reviewers.

References

African Atlas (2000) Ben Yahmed (sous la direction), Atlas de lAfrique. Les Editions du Jaguar, 22p

Balas N, Nicholson SE, Klotter D (2007) The relationship of rainfall variability in West Central Africa to sea surface temperature fluctuations. Int J Climatol 27:1335–1349

Bell MA, Lamb P (2006) Integration of waether system variability to multidecadal regional climate change: the West African Sudan Sahel Zone. J Clim 19:5343–5365

Biasutti M, Giannini A (2006) Robust Sahel drying in response to late 20th century forcings. Geophys Res Lett 33

Biasutti M, Held IM, Sobel AH, Giannini A (2008) SST forcings and Sahel Rainfall variability in simulations of the twentieth and twenty-first centuries. J Clim 21:3471–3486

Camberlin P, Janicot S, Poccard I (2001) Seasonality and atmospheric dynamics of the teleconnection between African rainfall and tropical SST: atlantic vs ENSO. Int J Climatol 21:973–1005

Champeaux JL, Tamburini A (1994) Zonage Climatique de la France à partir des séries de précipitations quotidiennes du Réseau Climatologique d'Etat. Pub Asso Int Climato 7:93–98

Corti S, Molteni F, Palmer TN (1999) Signature of recent climate change in frequencies of natural atmospheric circulation regimes. Nature 398:799–802

Crétat J, Richard Y, Pohl B, Rouault M, Reason CJC, Fauchereau N (2012) Recurrent daily rainfall patterns over South Africa and associated dynamics during the core of the austral summer. Int J Climatol 32:261–273

Czaja A, Van Der Vaart P, Marshall J (2002) A diagnostic study of the role of remote forcing in tropical atlantic variability. J Clim 15:3280–3290

Dreiser U (1994) Mapping of desert locust habitats in Africa using landsat thematic mapper data. Geojournal 32:55–60

Druyan LM (2010) Studies of 21st-century precipitation trends over West Africa. Int J Climatol 31(10):1415–1424

Folland CK, Palmer TN, Parker D (1986) Sahel rainfall and worldwide sea temperature, 190185. Nature 320:602–687

Fontaine B, Janicot S (1992) Wind field coherence and its variability over West Africa. J Clim 5:512–524

Giannini A, Biasutti M, Verstraete MM (2008) A climate model-based review of drought in the Sahel: desertification, the re-greening and climate change. Glob Planet Change 64:119–128

Giorgi F (2002) Variability and trends of sub-continental scale surface climate in the twentieth century. Part I: observation. Clim Dyn 18:675–691

Giorgi F, Francisco F (2000) Uncertainties in regional climate change prediction: a regional analysis of ensemble simulations with the HADCM2 coupled AOGCM. Clim Dyn 16:169–182

Gong X, Richman MB (1995) On the application of cluster analysis to growing season precipitation data in North America east of the Rockies. J Clim 8:897–931

Halpert MS, Ropelewski CF (1992) Surface temperature patterns associated with the Southern oscillation. J Clim 5:577–593

Hickey H, Weaver AJ (2004) The Southern Ocean as a source region for tropical atlantic variability. J Clim 17:3960–3972

Hoerling M, Hurrell J, Eischeid J, Phillips A (2006) Detection and attribution of twentieth-century northern and southern African rainfall change. J Clim 19:3989–4008

Hurrell JM (1995) Decadal trends in the North Atlantic oscillation regional temperatures and precipitation. Science 269:676–679

Janicot S (1992) Spatiotemporal variability of West African rainfall. Part I: regionalization and typings. J Clim 5:489–497

Jones PD, New M, Parker DE, Martin S, Rigor IG (1999) Surface air temperature and its changes over the past 150 years. Rev Geophys 37:173–199

Kaiser G (1994) A Friendly Guide to Wavelets. Birkhäuser, Basel

Kaptué TAT, Bégué A, Los SO, Boone AA, Daouda B (2010) A new characterization of the land surface heterogeneity over Africa for use in land surface models. J Hydrometeorol 12:1321–1336

Kaptué TAT, De Jong SM, Roujean JL, Favier C, Mering C (2011) Ecosystem mapping at the African continent scale using a hybrid clustering approach based on 1-km resolution multi-annual data from SPOT/VEGETATION. Clim Dyn 115:452–464

Mather PM (1976) Computational methods of multivariate analysis in physical geography. Wiley, New York

Mo KC (2000) Relationships between low frequency variability in the southern hemisphere and sea surface temperature anomalies. J Clim 13(20):3599–3610

Mo KC, Hakkinen S (2001) Interannual variability in the tropical Atlantic and linkages to the Pacific. J Clim 14:2740–2762

Mounier F, Janicot S, Kiladis G (2008) The West African monsoon dynamics. Part III: the quasi-Biweekly Zonal Dipole. Am Meteorol Soc 9:1911–1942

Muñoz-Diaz D, Rodrigo FS (2004) Spatio-temporal patterns of seasonal rainfall in Spain (1912–2000) using cluster and principal component analysis: comparison. Ann Geophys 22:1435–1448

Muñoz-Diaz D, Rodrigo FS (2006) Seasonal rainfall variations in Spain (1912–2000) and their links to atmospheric circulation. Atmos Res 81:94–110

New MG, Hulme M, Jones PD (1999) Representing twentieth century space time climate variability. Part I: development of a 1961–1990 mean monthly terrestrial climatology. J Clim 12:829–856

New MG, Hulme M, Jones PD (2000) Representing twentieth century space time climate variability. Part II: development of a 1901–1996 mean monthly terrestrial climatology. J Clim 13:2217–2238

Nicholson SE (1989) Rainfall variability in Southern Africa and its relationship to ENSO and the Atlantic and Indian Oceans. In:

Preprints oft he third international conference on southern hemisphere meteorology and oceanography (Buenos Aires, Argentina). American Meteorological Society, pp 366–367

Nicholson SE (1997) An analysis of the ENSO signal in the tropical Atlantic and western Indiand Oceans. Int J Climatol 17:345–375

Nicholson SE (2000) The nature of rainfall variability over Africa on time scales of decades to millenia. Glob Planet Change 26:137–158

Nicholson SE (2001) Climatic and environmental change in Africa during the last two centuries. Clim Res 17:123–144

Nicholson SE, Grist JP (2001) A conceptual model for understanding rainfall variability in the West African Sahel on interannual and interdecadal time scales. Int J Climatol 21:1733–1757

Nicholson SE, Kim J (1997) The relationship of the El Nino Southern Oscillation to African rainfall. Int J Climatol 17:117–135

Nicholson SE, Some B, Kone B (2000) An analysis of recent rainfall conditions in West Africa, including the rainy seasons of the 1997 El Niño and the 1998 La Niña years. J Clim 13:2628–2640

Nicholson SE, Barcilon AI, Chaila M (2008) An analysis West Africa dynamics using a linearized GCM. J Atmos Sci 65:1182–1203

Penlap EK, Christopher Matulla HS, Kamga FM (2004) Downscaling of GCM scenarios to assess precipitations changes in the little rainy season (Mach-June) in Cameroon. Clim Res 26:85–96

Rajagopalan B, Kushnir Y, Tourre YM (1998) Observed decadal midlatitude and tropical Atlantic climate variability. Geophys Res Lett 25:3967–3970

Robertson AW, Farrara JD, Mechoso CR (2003) Simulations of the atmospheric response to South Atlantic sea surface temperature anomalies. J Clim 16:2540–2551

Ropelewski CF, Halpert MS (1996) Quantifying southern oscillation-precipitation relationships. J Clim 9:1043–1059

Rotstayn LD, Lohmann U (2002) Tropical rainfall trends and the indirect aerosol effect. J Clim 15:2103–2116

Rowell DP, Folland CK, Mashell K, Ward MN (1995) Variability of summer rainfall over tropical North Africa (1906–92): observations and modelling. Q J R Meteorol Soc 121:669–704

Sarr B (2012) Present and future climate change in the semi-arid region of West Africa: a crucial input for practical adaptation in agriculture. Atmos Sci Lett 13(2):108–112

Sultan B, Janicot S (2003) The West African monsoon dynamics. Part II: the pre-onset and the onset of the summer monsoon. J Clim 16:3407–3427

Torrence C, Compo GP (1998) A practical guide to wavelet analysis. Bull Am Meteorol Soc 79(1):62–78

Tourre YM, Rajagopalan B, Kushnir Y (1999) Dominant patterns of climate variability in the Atlantic Ocean region during the last 136 years. J Clim 12:2285–2299

Venegas SA, Mysak LA, Straub DN (1997) Atmosphere-ocean coupled variability in the South Atlantic. J Clim 10:2904–2920

Wang G, Alo CA (2012) Changes in precipitation seasonality in West Africa predicted by RegCM3 and the impact of dynamic vegetation feedback. Int J Geophys Article ID 597205

Ward MN (1998) Diagnostic and short-lead time prediction of summer rainfall in tropical North Africa at interannual and multidecadal timescales. J Clim 11:3167–3191

Ward MN, Lamb PJ, Portis DH, El Hamly M, Sebbari R (1999) Climate variability in Northern Africa: understanding droughts in the Sahel and the Maghreb, beyond El Niño: decadal and interdecadal climate variability. In: Navarra A (ed) Navarra Antonio, Chap 6. Springer, Vienna, Austria, pp 119–140

Yepdo DZ, Monkam D, Lenouo A (2009) Spatial variability of rainfall regions in West Africa during the 20th century. Atmos Sci Lett 10:9–13

Zeng N, Neelin JD, Lau KM, Tucker CJ (1999) Enhancement of interdecadal climate variability in the Sahel by vegetation interaction. Science 286:1537–1540